

Kinetic, equilibrium and thermodynamic studies for adsorption of nickel ions onto husk of *Oryza sativa*

Shagufta Zafar^{a,b,†}, Muhammad Imran Khan^{b,c,t,*}, Majeda Khraisheh^d, Mushtaq Hussain Lashari^{e,*}, Shabnam Shahida^f, Muhammad Farooq Azhar^g, Prasert Prapamonthon^h, Muhammad Latif Mirza^b, Nasir Khalidⁱ

^aDepartment of Chemistry, The Government Sadiq College Women University, Bahawalpur 63000, Pakistan, email: shg_zf@yahoo.com

^bDepartment of Chemistry, The Islamia University of Bahawalpur, Bahawalpur 63100, Pakistan, emails: raoimranishaq@gmail.com (M.I. Khan), mlatifmirza@gmail.com (M.L. Mirza)

^cSchool of Chemistry and Material Science, University of Science and Technology of China, Hefei 230026, Anhui, PR. China

^dDepartment of Chemical Engineering, College of Engineering, Qatar University, Doha, Qatar, email: m.khraisheh@qu.edu.qa

^eDepartment of Zoology, The Islamia University of Bahawalpur, Bahawalpur 63100, Pakistan, email: mushtaqhary@gmail.com

^fDepartment of Chemistry, The University of Poonch, Rawalakot, Azad Jammu and Kashmir, Pakistan, email: shabnamshahida01@gmail.com

^gDepartment of Forestry and Range Management Bahauddin Zakariya University, Multan, Pakistan, email: faarooqazhar@yahoo.com

^hKing Mongkut's Institute of Technology Ladkrabang, Bangkok, Thailand, email: prasert.pr@kmitl.ac.th

ⁱChemistry Division, Pakistan Institute of Nuclear Science and Technology, PO Nilore, Islamabad, Pakistan, email: nasirk1953@gmail.com

Received 8 February 2019; Accepted 29 June 2019

ABSTRACT

This research focus onto batch adsorption of nickel ions (Ni(II)) onto husk of *Oryza sativa* (HOS) from aqueous solution at room temperature. Several techniques such as Fourier transform infrared, scanning electron microscopy and energy dispersive X-ray were employed to confirm adsorption of Ni(II) onto HOS. The effect of operational parameters such as contact time, amount of adsorbent, initial concentration of metal ions, temperature and pH on the percentage removal of Ni(II) was evaluated. The removal of Ni(II) was 62.32% under optimum amount of adsorbent (0.3 g) at room temperature. Adsorption kinetics study has exhibited that experimental data fitted well to pseudo-second-order kinetic model. Linear and nonlinear forms of Langmuir, Freundlich and Dubinin-Radushkevich isotherms were used to analyse experimental data and results showed that adsorption data fitted well to nonlinear and linear form of adsorption isotherms. Adsorption thermodynamic study has indicated that adsorption of Ni(II) onto HOS was an endothermic and spontaneous process.

Keywords: Nickel ions; Adsorption; Husk of *Oryza sativa*; Isotherms; Thermodynamics

1. Introduction

There is an essential requirement to provide safe drinking water to its people for all properly functioning societies. Contamination of water with toxic metals such as mercury

(Hg), nickel (Ni), cadmium (Cd), arsenic (As), chromium (Cr), thallium (Tl), lead (Pb) copper (Cu), cobalt (Co), iron (Fe), magnesium (Mg), manganese (Mn), molybdenum (Mo), selenium (Se), zinc (Zn) and aluminum (Al) in ground water are of major concerns for its hazardous effect on the

* Corresponding authors.

† Both authors contributed equally to this work

environment [1]. Heavy metal pollution in water is very high in areas where mining, smelters, metal processing refineries, wood preservation and paper processing facilities are located. Human exposure to heavy metals as well as public concern for the associated health risks have both risen dramatically as a result of an exponential increase of their use in these various applications.

Nickel (Ni(II)) is one of the toxic heavy metals in wastewater, which has been supported significant observations because of its carcinogenicity, toxicity, and cumulative adverse properties. Ni(II) pollution which stem from metal smelting, mining, metal processing, and battery manufacturing [2,3], is concentrated and cumulated in living organisms. High concentration of Ni(II) in human beings would lead to serious results having headache, heart damage and even cancer [4]. Thus, it is important to eliminate Ni(II) from the water and wastewater for protecting the public safe and the environment. Recently, many methods have been applied in the removal of Ni(II), such as adsorption [5], chemical precipitation [6], ultra-filtration [7], membrane filtration [8], ion exchange [9] and so on. However, most of the methods also have issues, namely high cost, ineffectiveness at low concentration and inapplicability for different types of pollutants. Of all the methods, adsorption is one of the most effective, economic and convenient technology [10].

Several investigators carried out the scavenging of Ni(II) from aqueous media. The use of agro-waste for the remediation of wastewater is growing nowadays. There are a number of agro-wastes which were successfully used for removal of Ni(II) from aqueous medium. *Moringa oleifera* seeds [11], sawdust [12–14], fruit peelings [15,16], sugarcane bagasse [17], acacia bark [18], ground nut shell [19], *Rhizoclonium tortuosum* (RT) [20], ultrasonic-modified jujube seeds (UMJS) [21], coconut husk [22], leaf powder [23] were reported in literature and proved to be an efficient adsorbents for Ni(II) because of functional groups present on them. Modified sand [24] and clay [25] were used as an adsorbents for Ni(II) adsorption from wastewater. Bentonite and zeolite [26,27], montmorillonite [28], laterite [29] and clinoptilolite [30] were some of the natural clays used as adsorbent. Moreover, *Cassia fistula* seed based adsorbent was also used for removal of Ni(II) from aqueous solution [31]. Activated carbon has been proved as an excellent adsorbent for heavy metals but it is expensive. Therefore, a lot of work has been done for the preparation of activated carbon from various agro-wastes [32–34]. Its applications for Ni(II) remediation from aqueous media has been reported in literature. Scavenging of Ni ions by multi-walled carbon nanotubes were carried out and reported by various researchers [35–37].

Our previous work have reported the use of different plant leaves [38–41] and anion exchange membrane (AEMs) [42–47] for removal of dyes from aqueous at room temperature. This work will use husk of *Oryza sativa* (HOS) as an effective adsorbent for the removal of Ni(II) from aqueous solutions at room temperature. As Pakistan includes in the big producer of rice (5.2 million tons annually) and its husk which forms 20%–23% of the whole rice grain is supposed as undesirable waste material that actually poses a disposal issue for mill owners [48,49]. Its basic composition is proteins, cellulose, hemicellulose and lignin, having hydroxyl and carboxyl functional groups available to interact with

cations [50,51]. Due to these properties, HOS will be used as an adsorbent for removal of Ni(II) from aqueous solution. Therefore, we report batch adsorptive removal of Ni(II) by HOS from aqueous solution in detail at room temperature. The influence of operating parameters such as contact time, amount of adsorbent, initial concentration of metal ions, temperature and pH onto percentage removal of Ni(II) was evaluated in detail. Experimental data for adsorption of Ni(II) onto HOS was subjected to several adsorption kinetic models, linear and nonlinear forms of isotherms and thermodynamics.

2. Experimental section

2.1. Adsorbent

All experimental work was conducted from the same batch of rice to eliminate any effect of seasonal variation in the rice sample. The husk of basmati rice (botanical name: *Oryza sativa*) was obtained from a rice mill, Punjab and Pakistan. The required samples were thoroughly washed with water to remove dust particles and were oven dried at 80°C till constant weight was obtained. The dried husk was stored in a pre-cleaned airtight container and was used without any physical or chemical pre-treatment. The chemical analysis of husk samples of basmati rice was carried out by employing neutron activation analysis (NAA) and atomic adsorption spectrometry (AAS) for their trace metal contents and obtained results have been reported elsewhere [52]. The results showed that the amount of metals such as Na, K, Pb and Fe were present in µg/g of sample. Silica contents were found to be 18.27 (0.62%) of HOS. The trace amount of elements present in HOS were analysed by adopting standard procedure such as AAS and NAA. The adsorption capacities of different adsorbents for Ni(II) are given in Table 1.

2.2. Reagents

The temperature of solutions was maintained by dipping the culture tube in water bath of Gallen kamp thermo stirrer (UK) for thermodynamic studies. The precision of temperature in water bath was $\pm 0.1^\circ\text{C}$. All the reagents used were of analytical grade and used without further modifications. Deionized water was used throughout this work.

2.3. Adsorption experiment

A known amount of HOS was taken into a 25 cm³ secured cap culture tube and a fixed amount of stock radio-tracer with known amount of nickel concentration solution was added. Subsequently, the contents were equilibrated on a wrist-action mechanical shaker (Vibromatic, USA) at a rate of 500 rpm for specific time. Then it was centrifuged at 5,000 rpm for phase separation and the supernatant solution was withdrawn for activity measurement. The radio-activity of solutions before (A_0) and after (A_t) equilibrium was measured with a NaI well type scintillation counter (Canberra Inc., Germany) coupled with a counter-scaler (Nuclear Chicago). A volume of 1.0 cm³ was usually used to measure the activity. All experiments were conducted at ambient temperature. The percentage removal of nickel

Table 1
Adsorption capacities of Ni(II) for different adsorbents

Adsorbents	Capacity (mg/g)	References
EDTA modified silica gel	19.62	[53]
DTPA modified silica gel	16.97	[53]
Arca shell	3.538	[54]
Modified riverbed sand	0.13	[55]
Saccharum bengalense	0.319	[56]
Mod. <i>Ceiba pentandra</i> hulls	10.55	[57]
Holly sawdust	7.87	[12]
AC sugarcane bagasse pith	2.206	[58]
Palm shell AC	0.607	[33]
Waste tea leaves	0.934	[59]
Rice husk ash	0.0813	[60]
Modified coconut husk	9.206	[22]
Rice husk	0.18	[61]
Sawdust	0.11	[14]
Mosambi fruit peelings	23.92	[15]
Lignocellulose/montmorillonite	81.34	[62]
Microalga <i>Rhizoclonium hookeri</i>	65.81	[63]
Husk of <i>Oryza sativa</i>	62.501	Present study

ions from aqueous solution was measured by employing the following relation:

$$\% \text{ adsorption} = \frac{A_i - A_f}{A_i} \times 100 \quad (1)$$

where A_i and A_f are initial and final adsorption of metal ions (counts/min) into the solution respectively.

2.4. Characterization

2.4.1. Morphology

Morphology of HOS was investigated by field emission scanning electron microscope (FE-SEM, Sirion200, FEI Company, USA).

2.4.2. Energy dispersive X-ray (EDX) analysis

The adsorption of Ni(II) onto HOS was confirmed by energy dispersive X-ray (EDX) analysis.

2.4.3. Fourier transform infrared (FTIR) analysis

Fourier transform infrared (FTIR) analysis was carried out by using the technique attenuated total reflectance with FTIR spectrometer (Vector 22, Bruker) having resolution of 2 cm^{-1} and a total spectral range of $4,000\text{--}400 \text{ cm}^{-1}$.

3. Results and discussion

3.1. Characterization of adsorbent

The HOS used was characterized for various physico-chemical properties such as moisture and ash contents,

porosity, bulk density, pH_{pzc} and Brunauer-Emmett-Teller surface area by using standard procedures and determined values were reported to be 2.61%, 20.11%, 70.66% and 0.305 g/cm^3 , 5.84 and $1.03 \text{ m}^2/\text{g}$, respectively and is reported [64]. The elemental analysis of basmati HOS samples was also carried out employing NAA and AAS for their trace metal contents and results have been reported elsewhere [52].

3.2. Scanning electron microscopy (SEM) and EDX test

Morphology of HOS was illustrated by employing scanning electron microscopy (SEM) in detail. Fig. 1 represents the SEM micrographs of HOS before and after adsorption of Ni(II). It is clear that the surface of HOS was irregular and rough with many loops and humps. The pores can be classified according to their sizes as primary micropores 0.8 nm , secondary micropores $0.8\text{--}2 \text{ nm}$, mesopores $2\text{--}50 \text{ nm}$ and macropores 50 nm with width sizes. The determined pore size present on the surface of HOS was in a range of $100\text{--}180 \text{ nm}$ confirming macro-porous structure of adsorbents. As shown in Fig. 1 that after adsorption of Ni(II), the surface morphology of the adsorbent was changed. The pores and grooves were filled which were present before metal ions adsorption and decrease in surface heterogeneity was observed resulting into the smooth surface. Ionic radii of nickel is 0.074 nm , which is much smaller than the pore size present on HOS, ($100\text{--}180 \text{ nm}$), enabling adsorption of Ni(II) through pore diffusion.

The presence of energy peak decided the adsorption of Ni(II) which was illustrated by EDX analysis of HOS and shown in Fig. 2. The peaks for nickel energy lines were present in the range of 0.70 to 8.10 keV by EDX pattern. It showed the successful adsorption of Ni(II) onto HOS.

3.3. Fourier transform infrared

The adsorption of Ni(II) onto HOS was also proved by FTIR analysis of virgin and Ni(II) loaded HOS samples. Fig. 3a depicts the FTIR spectrum of virgin HOS. The peaks at $1,737.8$; $1,435.6$ and $1,365.4 \text{ cm}^{-1}$ are attributed with C=O stretching, OH bending of the adsorbed H_2O and aliphatic C–H bending respectively [65]. The peaks at $1,217.0$; $1,365.4$; $1,737.8$ and $1,027.4 \text{ cm}^{-1}$ are due to carboxyl group on HOS whereas the peaks at $1,208\text{--}1,230 \text{ cm}^{-1}$; $1,367\text{--}1,371 \text{ cm}^{-1}$; $1,740$ and $1,029 \text{ cm}^{-1}$ for carboxyl group [66,67]. The characteristic absorption band at $3,400\text{--}3,200 \text{ cm}^{-1}$ is assigned for surface O–H stretching whereas aliphatic C–H stretching had a broad band at $2,921\text{--}2,851 \text{ cm}^{-1}$. Moreover, the peak at $10,74.0 \text{ cm}^{-1}$ corresponds to anti-symmetric stretching vibration of Si–O, whereas at 476.2 cm^{-1} representing the bending vibration of Si–O–Si bond [66,68,69].

After adsorption of Ni(II) onto HOS, the changes in the intensities or positions of functional groups were important to look into FTIR spectrum, which were associated for adsorption of Ni(II). Fig. 3b depicts FTIR spectrum of Ni(II) loaded HOS. For Ni(II) loaded HOS, the peaks shifted to $2,910.1$; $1,734.7$; $1,646.8$ and $1,372.8 \text{ cm}^{-1}$, whereas the intensities of $1,734.7$; $1,216.3$ and $1,027.7 \text{ cm}^{-1}$ were observed after adsorption of Ni(II) onto HOS. It showed the successful adsorption of Ni(II) onto HOS.

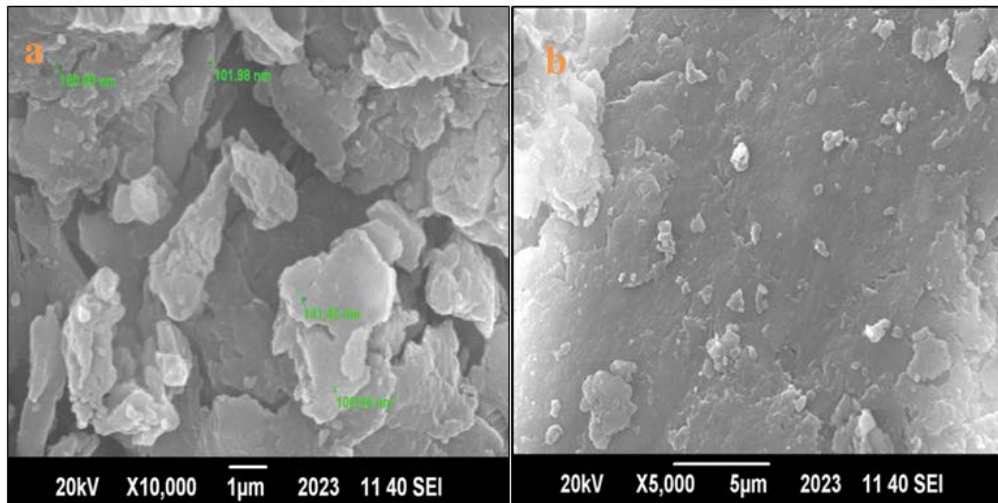


Fig. 1. SEM image of (a) virgin and (b) Ni(II) loaded husk of *Oryza sativa*.

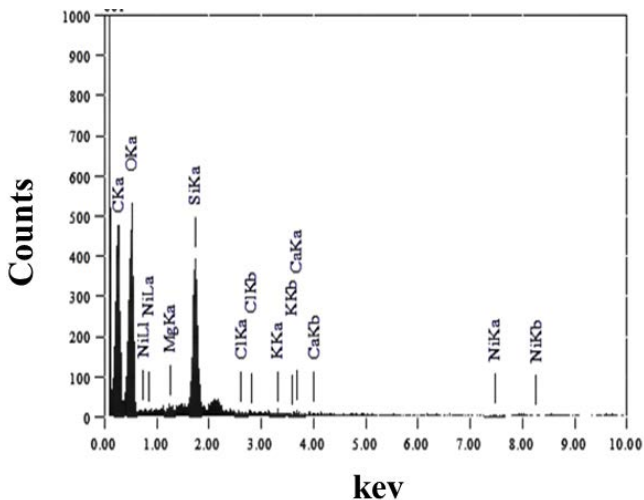


Fig. 2. Energy dispersive X-ray image of Ni(II) loaded husk of *Oryza sativa*.

3.4. Effect of operational parameters

The effect of contacts time, mass of adsorbent, initial concentration of metal ions, temperature and pH onto percentage removal has been evaluated in detail. These are as follows:

3.4.1. Effect of contact time

The effect of contact time onto the percentage removal of Ni(II) was investigated by keeping amount of HOS, concentration of Ni(II), shaking speed and temperature constant and attained results are shown in Fig. 4. It can be seen that the percentage removal of Ni(II) is found to be increased from 42.99% to 62.32% with contact time from aqueous solution. It was fast in start and then there was no large change into the percentage removal of Ni(II), after this equilibrium was established and no further large enhancement into the removal was observed with contact

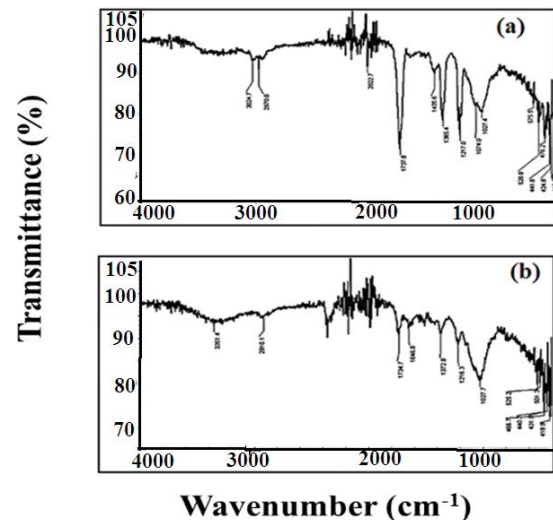


Fig. 3. FTIR spectrum of (a) virgin RH and (b) Ni(II) loaded husk of *Oryza sativa*.

time. It was rapid in the beginning because of presence of several empty sites onto HOS and interaction was developed between Ni(II) and adsorption sites. The adsorption slowed down when all the surface sites were occupied due to movement of metal ions deep into interior pores of HOS. Another reason could be that several vacant sites supported rapid adsorption and when these sites were occupied than there was a competition for lesser remaining sites for the metals ions to be adsorbed which slowed down the rate of adsorption until equilibrium was established. The equilibration time for Ni(II) was 15 min which is much less than reported equilibrium time 50 and 250 min for Ni(II) by *Ceiba pentandra* Hulls in literature for Ni(II) [57].

3.4.2. Effect of amount of adsorbent

The influence of amount of HOS onto the percentage removal of Ni(II) was studied keeping contact time, initial

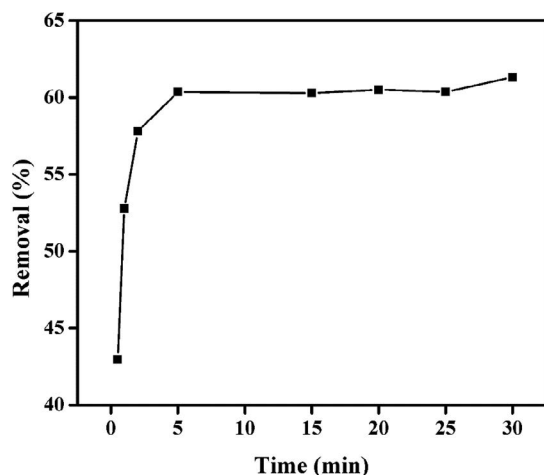


Fig. 4. Effect of contact time onto adsorption of Ni(II) onto husk of *Oryza sativa*, initial concentration of metal ion = 20.26 mg/L, amount of adsorbent = 0.3 g, volume of adsorbate = 10 mL, temperature = RT.

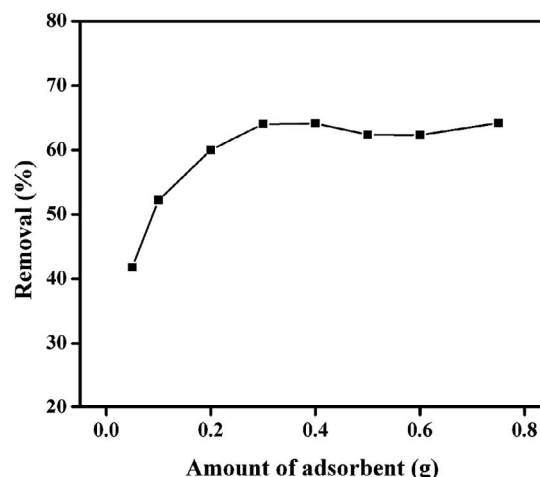


Fig. 5. Effect of amount of husk of *Oryza sativa* onto adsorption of Ni(II), contact time = 30 min, initial concentration of metal ion = 20 mg/L, volume of adsorbate = 10 mL, Temperature = RT.

concentration of metal ions, temperature and shaking speed constant. The attained results are represented in Fig. 5. The percentage removal of Ni(II) is found to be enhanced from 41.80% to 64.20% with increasing mass of HOS from 0.05 to 0.75 g. The percentage removal of Ni(II) was increased up to 0.3 g and further increase in amount of HOS has no major effect onto the percentage removal. Similar results were reported in literature [20,39,48].

3.4.3. Effect of initial concentration

The effect of initial concentration of metal ion onto the percentage removal was evaluated keeping other endowments constant. Fig. 6 represents the effect of initial concentration onto the removal of Ni(II) by HOS from aqueous solution. It has been observed that the percentage removal of Ni(II) is found to be decreased from 61% to 31% with enhancing initial concentration of Ni(II) into aqueous solution. The same trend was observed for adsorption of methyl orange onto microwave assisted sawdust from aqueous solution [70]. Some of the metal ions were left unadsorbed at higher initial concentration of metal ions because of saturation of adsorption sites. At low concentration of metal ions more binding sites were available. The number of ions competing for present binding sites onto HOS was enhanced with increasing the concentration of metal of ions. Similar results was reported in our previous work [41,47].

3.4.4. Effect of temperature

The influence of temperature onto the percentage removal of Ni(II) was evaluated keeping contact time, amount of HOS, concentration of Ni(II) and shaking speed constant and attained results are denoted in Fig. 7. There was an increase into adsorption of metal ions for all adsorbate–adsorbent systems with a rise in temperature which indicates higher adsorption at elevated temperatures. It can be seen that the percentage removal of Ni(II) from aqueous

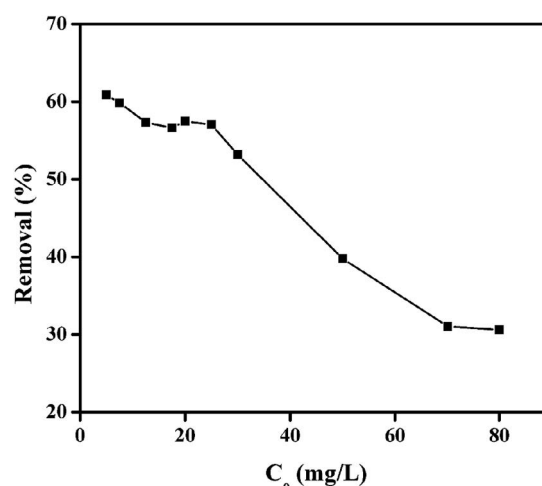


Fig. 6. Effect of initial concentration onto adsorption of Ni(II), contact time = 15 min, amount of adsorbent = 0.3 g, volume of adsorbate = 10 mL, Temperature = RT.

solution is found to be enhanced from 59.4% to 65% with rise in temperature. The increase in adsorption of Ni(II) by increasing temperature may be either due to acceleration of some originally slow adsorption steps or to the creation of some new active sites on the surface of the adsorbent. Similar results was reported in our previous work [38,39].

3.4.5. Effect of pH

The pH of adsorption medium is an important parameter which governs metal ions adsorption on different adsorbents. The pH effect on heavy metals adsorption from aqueous media had been reported by many workers [71–74]. It is well known fact that pH of adsorbing solution affects the metal ions solubility and chemical speciation and counter ions concentration on the functional groups of the adsorbents. It is fact that in aqueous media the metal species

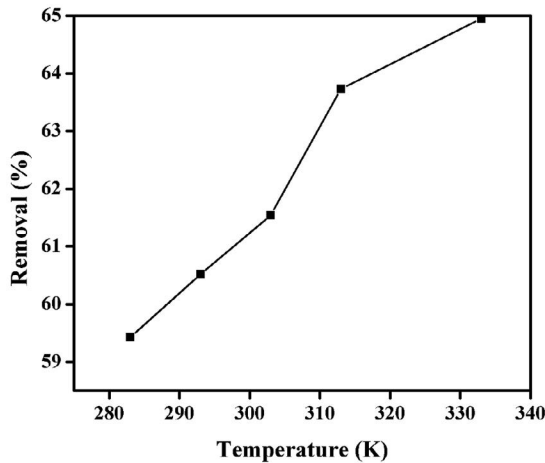


Fig. 7. Effect of temperature onto adsorption of Ni(II), contact time = 15 min, initial concentration of metal ions = 20 mg/L, amount of adsorbent = 0.3 g, volume of adsorbate = 10 mL.

are present as M^{+n} , $M(OH)^{+(n-1)}$, $M(OH)_2^{+(n-2)}$ etc. The pH not only influences the metal ions speciation but also charges on the sorption sites of adsorbent [73,75,76]. It is very important to consider the metal solution chemistry and functional groups ionic states on the adsorbent in different pH solutions. More concentration of H^+ ions in the medium is present at low pH resulting in the protonation of adsorbent. Thus, H^+ ions occupy the adsorption sites before the attack of metal ions on them and as a result forming adsorbent as positively charged species [77]. The positive character will decrease with rise in the pH. Fig. 8 shows the pH effect on the adsorption of nickel (Ni^{2+}) ions. The variation in adsorption of Ni^{2+} with change in solution pH revealed that more adsorption occurred as pH increase. As the pH of the system increased, the negatively charged sites were increased which favors the metal ions adsorption due to electrostatic attraction. The maximum removal of Ni^{2+} occurred at pH 10.

3.5. Adsorption kinetics

3.5.1. Pseudo-first-order model

The linearized form of the Lagergren pseudo-first-order rate equation is given as [46]:

$$\log(q_e - q_t) = \log q_e - \frac{k_1 t}{2.303} \quad (2)$$

where q_e and q_t represents the amount of the adsorbed Ni(II) at equilibrium and time t respectively and k_1 (/min) is the rate constant of pseudo-first-order model. The plot of $\log(q_e - q_t)$ vs. t for adsorption of Ni(II) onto HOS is depicted in Fig. 9. The values of k_1 and q_e were calculated from slope and intercept and are given in Table 2. The plot are linear, however the linearity of these curves does not necessarily assure the mechanism due to the inherent disadvantage of correctly estimating equilibrium adsorption capacity [78]. The value of correlation coefficient ($R^2 = 0.765$) was less than unity for adsorption of Ni(II) onto HOS. Further, the difference

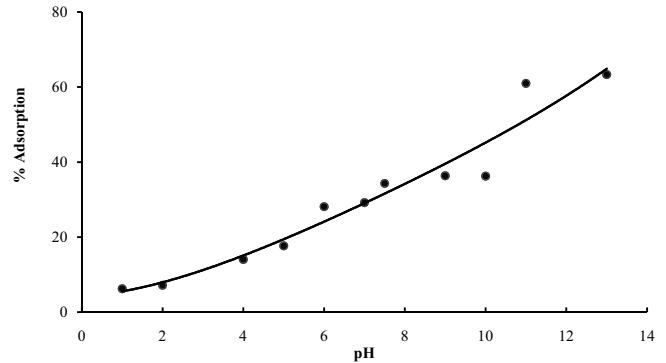


Fig. 8. Plot of pH for adsorption of Ni(II) onto husk of *Oryza sativa*.

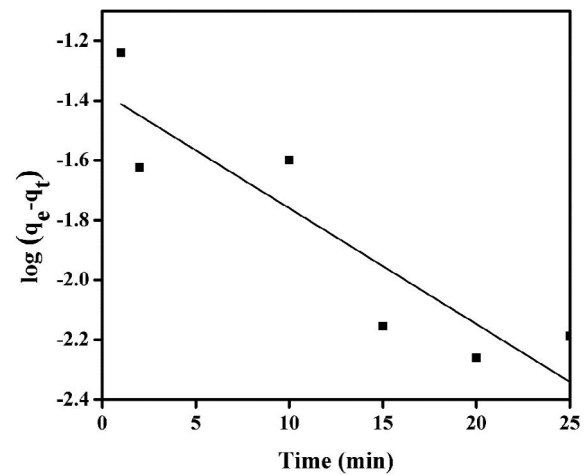


Fig. 9. Pseudo-first-order kinetics for adsorption of Ni(II) onto husk of *Oryza sativa*.

between experimental adsorption capacity ($q_{e,exp}$) and calculated adsorption capacity values ($q_{e,cal}$) is very large for adsorption of Ni(II) onto HOS. Hence adsorption of Ni(II) onto HOS does not obey pseudo-first-order kinetics.

3.5.2. Pseudo-second-order model

The linearized form of pseudo-second kinetic model is shown as [47]

$$\frac{t}{q_t} = \frac{1}{k_2 q_e^2} + \frac{t}{q_e} \quad (3)$$

where k_2 (g/mg min) is the rate constant of pseudo-second-order model. The plot of t/q_t vs. t for adsorption of Ni(II) onto HOS is represented in Fig. 10. The adsorption capacity (q_e) can be calculated from slope of plot of t/q_t vs. t and is represented in Table 2. This is in good agreement with the experimental value (0.42 mg/g) for adsorption of Ni(II) onto HOS. Further, the value of correlation coefficient is close to unity ($R^2 = 0.999$) which denotes that the experimental data fitted well to pseudo-second-order kinetics.

Table 2
Pseudo-first-order, pseudo-second-order and Elovich model rate constants. (q_e : mg/g; k_1 : (min⁻¹); k_2 : g/mg min; α : mg/g min; β : g/mg)

	Pseudo-first order	Pseudo-second-order	Elovich model		
$q_{e,exp}$	0.41	q_e	0.41	A	5,6471.5
$q_{e,cal}$	0.042	k_2	8.51	B	662.25
$k_1 \times 10^{-2}$	3.9	–	–	–	–
R^2	0.765	R^2	0.999	R^2	0.643

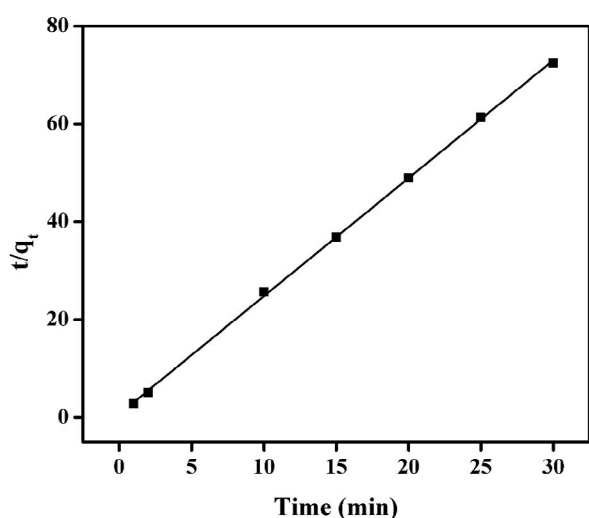


Fig. 10. Pseudo-second-order kinetics for adsorption of Ni(II) onto husk of *Oryza sativa*.

3.5.3. Elovich model

The most interesting model to explain the activated chemisorption is the Elovich equation [45].

$$q_t = \frac{1}{\beta} \ln(\alpha\beta) + \frac{1}{\beta} \ln t \quad (4)$$

where α (mg/g min) and β (g/mg) are constant of Elovich model. The endowment α is considered as initial adsorption rate (mg/g min) and β is related to the extent of surface coverage and activation energy for the chemisorption. Fig. 11 shows the graphical representation of Elovich model for adsorption of Ni(II) onto HOS. The values of α and β were determined from intercept and slope of plot and attained results are given in Table 2. The value of correlation coefficient ($R^2 = 0.643$) was lower than that of pseudo-second-order model.

3.5.4. Liquid film diffusion model

The liquid film model is represented as [45].

$$\ln\left(1 - \frac{q_t}{q_e}\right) = -K_{fd}t \quad (5)$$

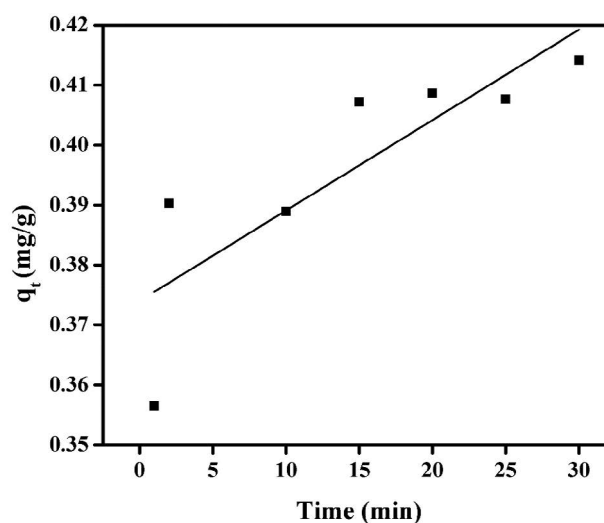


Fig. 11. Elovich model for adsorption of Ni(II) onto husk of *Oryza sativa*.

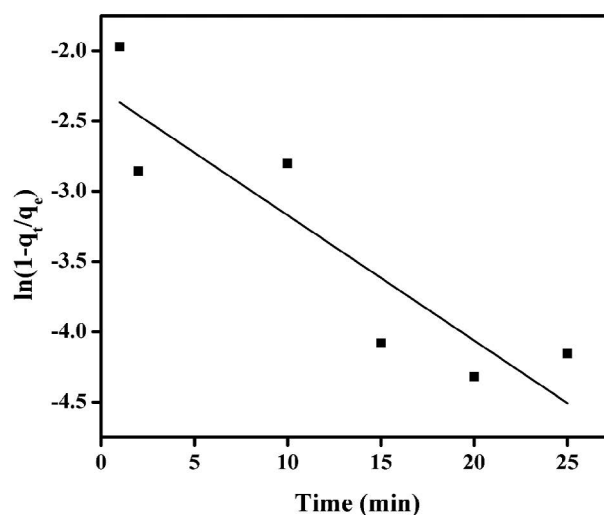


Fig. 12. Liquid film diffusion model for adsorption of Ni(II) onto husk of *Oryza sativa*.

where K_{fd} is liquid film diffusion rate constant. Fig. 12 represents the plot of $\ln(1 - q_t/q_e)$ vs. t is a straight line for liquid film model. The value of K_{fd} was measured from slope of plot and is shown in Table 3. The value of correlation coefficient ($R^2 = 0.765$) is lower than pseudo-second-order model. The inability of the plot to pass through the origin indicates that it was not only the rate determining but there also involves other mechanisms. It exhibits that liquid film diffusion model cannot be sufficient to explain the experimental data and other models are also required.

3.5.5. Modified Freundlich Equation

The modified Freundlich equation was originally developed by Kuo and Lotse [47].

$$q_t = kC_0 t^{1/m} \quad (6)$$

Table 3
Liquid film diffusion model, modified Freundlich equation and Bangham equation rate constant (K_d : (min⁻¹); K : L/g min; k_0 : mL/g/L)

Liquid film diffusion model	Modified Freunlich equation	Bangham equation	
K_{td}	0.089	M 28.10	k_0 0.18
C_{td}	2.28	K 1,076.70	A 0.036
R^2	0.765	R^2 0.786	R^2 0.787

where C_0 is the initial concentration (mg/L) of metal ions, k is apparent adsorption rate constant (L/g min), and m is the Kuo-Lotse constant. The values of k and m were employed to evaluate the influence of Ni(II) surface loading and ionic strength on the adsorption process. The linear form of modified Freundlich equation is given as:

$$\ln q_t = \ln(kC_0) + \frac{1}{m} \ln t \tag{7}$$

Fig. 13 shows the graphical representation of modified Freundlich equation. The values of m and k were measured from slope and intercept of plot of $\ln t$ vs. $\ln q_t$, and are represented in Table 3. Further, the value of correlation coefficient ($R = 0.786$) is lower than pseudo-second-order kinetic model.

3.5.6. Bangham Equation

Bangham equation [47] is represented as

$$\log \log \left(\frac{C_0}{C_0 - q_t m} \right) = \log \left(\frac{k_0 m}{2.303V} \right) + \alpha \log t \tag{8}$$

Fig. 14 shows the plot of $\log \log (C_0/C_0 - q_t m)$ vs. $\log t$ for adsorption of Ni(II) onto HOS. The values of α and m were calculated from slope and intercept and are represented in Table 3. The double logarithmic plot did not give linear curves for Ni(II) adsorption onto HOS indicating that the diffusion of adsorbate into pores of the adsorbent is not the only rate controlling step [79,80]. It may be that both HOS and pore diffusion were crucial to different extent in the adsorption of Ni(II).

3.6. Adsorption isotherms

Proper quantification of adsorption method is needed for application of adsorption process on the commercial level. Adsorption equilibrium is essential for the analysis and design of adsorption process it gives fundamental data of physicochemical method for investigating the applicability of the process as a unit operation. To obtain it, experimental data was studied employing Langmuir, Freundlich and Dubinin-Radushkevich (D-R) adsorption isotherms.

3.6.1. Langmuir sorption isotherm

The Langmuir isotherm has been used by many workers for adsorption analysis of several systems [81]. Langmuir

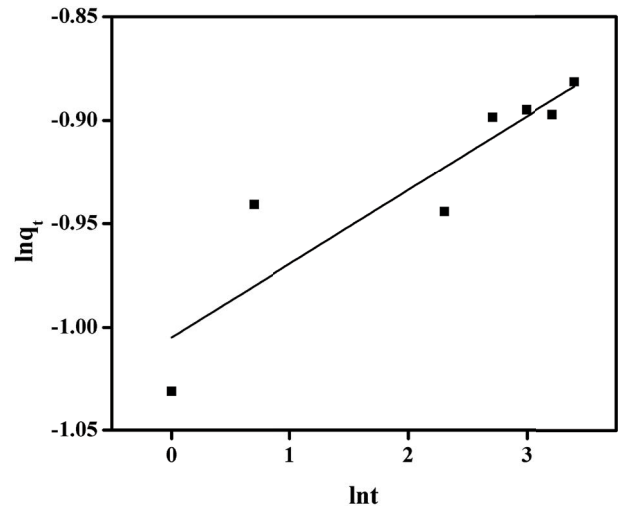


Fig. 13. Modified Freundlich equation plot between $\ln t$ vs. $\ln q_t$ for adsorption of Ni(II) onto husk of *Oryza sativa*.

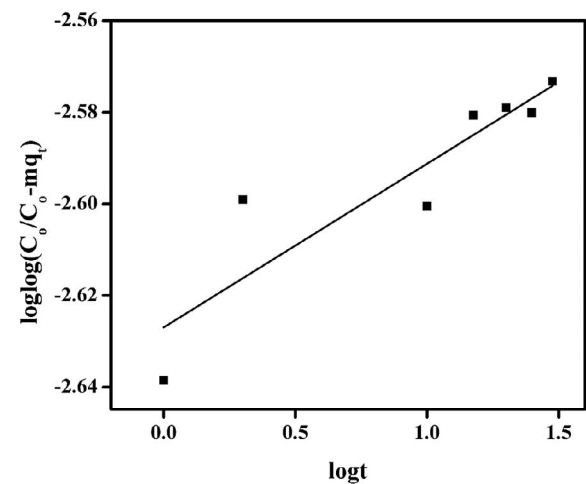


Fig. 14. Bangham equation plot between $\log t$ vs. $\log \log(C_0/C_0 - m q_t)$ for adsorption of Ni(II) onto husk of *Oryza sativa*.

model considers homogeneity of the adsorbing surface and no interactions between adsorbed species containing uniform energies of adsorption onto surface and no trans-migration of adsorbate species in plane of the surface. The difference in adsorption capacities of two adsorbents for same adsorbate is believed to be high because of physicochemical properties of them or the chemistry of solution having adsorbing species.

Langmuir adsorption isotherm may be shown as:

$$C_{ads} = \frac{Q_m K_L C_e}{1 + K_L C_e} \tag{9}$$

The above nonlinear Langmuir isotherm can be linearized as:

$$\frac{C_e}{C_{ads}} = \frac{1}{Q_m K_L} + \frac{C_e}{Q_m} \tag{10}$$

where C_{ads} is the amount adsorbed per unit mass onto adsorbent at equilibrium (mol/g), and C_e is the metal ions concentration of solution (mol/L) at equilibrium. The constant Q_m is monolayer adsorption capacity (mol/g) and K_L (L/mol) is related to energy of adsorption. Generally Q_m and K_L are functions of pH, ionic media and ionic strength. The value of Q_m for Ni(II) was computed by nonlinear and linear forms of Langmuir isotherm. Wavemetrics IGOR Pro 6.1.2 software was employed for the determination of isotherm endowments while employing non-linear equations. The non-linear form of Langmuir isotherm model for adsorption of Ni(II) onto HOS is represented in Fig. 15 and obtained constants are given in Table 4. Similarly, the linearized form of Langmuir isotherm model for adsorption of Ni(II) onto HOS is shown in Fig. 16 and obtained parameters are given shown in Table 5. To compare the application of different forms of the used models, the regression coefficient 'R²' and Chi-square test 'χ²' were employed as calculating tools for the best-fit of adsorption isotherm equations which may be measured by the following equations:

$$R^2 = \frac{\sum(C_{ads,cal} - \hat{C}_{ads,exp})^2}{\sum(C_{ads,cal} - \hat{C}_{ads,exp})^2 + \sum(C_{ads,cal} - C_{ads,exp})^2} \quad (11)$$

$$\chi^2 = \sum \frac{(C_{ads} - C_{ads,m})^2}{C_{ads,m}} \quad (12)$$

where $C_{ads,cal}$ is calculated adsorption at time t (mol/g), $\hat{C}_{ads,exp}$ is average of $C_{ads,exp}$ (mol/g), $C_{ads,exp}$ is experimental adsorption at time t (mol/g), and $C_{ads,m}$ is calculated equilibrium capacity from the model (mol/g). The computed value of 'R²' for linear equations is represented in Table 5 and Chi-square 'χ²' for nonlinear equation is given in Table 4. The similarity of data attained from a non-linear model is generally confirmed by comparison with the experimental data, χ² would be a smaller number and vice versa, whereas for linear models, maximum value of 'R²' is supposed to be more favorable.

A crucial characteristic of a Langmuir isotherm can be represented in terms of a dimensionless constant 'separation factor' parameter, 'R_L' that is employed to determine if an adsorption system is "favorable" or "unfavorable" and can be shown as follows:

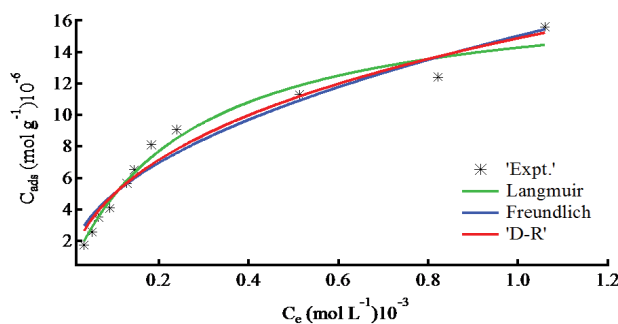


Fig. 15. Nonlinear plots of Langmuir, Freundlich and D-R isotherms for adsorption of Ni(II) onto husk of *Oryza sativa*.

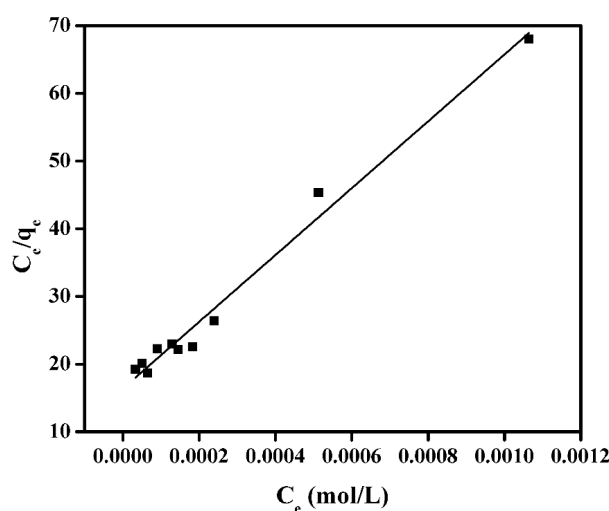


Fig. 16. Linear form of Langmuir isotherm for adsorption of Ni(II) onto husk of *Oryza sativa*.

$$R_L = \frac{1}{(1 + K_L C_0)} \quad (13)$$

where K_L is the Langmuir adsorption equilibrium constant (L/mol). The value of R_L represents adsorption process to be either unfavorable ($R_L > 1$), linear ($R_L = 1$), favorable ($0 < R_L < 1$) or irreversible ($R_L = 0$).

Table 4
Langmuir, Freundlich and Dubinin-Radushkevich isotherms parameters by nonlinear method (Q_m : mol/g; K_F : mol/g; β : mol²/J²; K_L : L/mol)

Isotherms	Parameters	χ ²
Langmuir isotherm	Q_m	K_L
	1.82×10^{-5}	3,678
Freundlich Isotherm	K_F	N
	$(4.106 \pm 1.310) \times 10^{-4}$	2.088 ± 0.181
	C_m	B
D-R Isotherm	$(6.097 \pm 0.841) \times 10^{-5}$	$(4.915 \pm 0.377) \times 10^{-3}$
	$E = 10.086 \pm 0.77$	7.4×10^{-12}

Table 5
Langmuir, Freundlich and Dubinin-Radushkevich isotherms parameters by linear method (Q_m : mol/g; K_f : mol/g; β : mol²/J²)

Isotherms	Parameters	R^2
Langmuir isotherm	Q_m 2.02×10^{-5} $R_L = 0.163-0.778$	K_L 3,014 0.9851
Freundlich Isotherm	K_f $1.064 \times 10^{-3} \pm 7.120 \times 10^{-5}$	N 1.675 ± 0.147 0.935
D-R Isotherm	C_m $(9.00 \pm 0.185) \times 10^{-5}$ $E = 9.28 \pm 0.640$	B $(5.773 \pm 0.397) \times 10^{-3}$ 0.959

The values of R_L for adsorption of Ni(II) was measured from Langmuir constant K_L and initial concentrations of metal ion and results are summarized in Table 5 which established that adsorption of Ni(II) onto HOS was favorable representing by the fractional values of R_L between one and zero.

3.6.2. Freundlich isotherm model

Freundlich isotherm was given by Herbert F. Freundlich which is given as follows:

$$C_{\text{ads}} = K_f C_e^{1/n} \quad (14)$$

The linearized form of Freundlich isotherm is represented as:

$$\log C_{\text{ads}} = \log K_f + \frac{1}{n} \log C_e \quad (15)$$

where K_f and n are Freundlich constants representing adsorption capacity and adsorption intensity respectively. The good fit of adsorption data to Freundlich isotherm shows that there is almost no limit to the quantity adsorbed and multilayer adsorption will happen. The linear form of Freundlich adsorption isotherm for adsorption of Ni(II) onto HOS is depicted in Fig. 17 and calculated endowments are shown in Table 5. The nonlinear form of Freundlich isotherm was also applied on experimental data and obtained values of K_f and n are given in Table 4. The value of n proclaims the heterogeneous surface of the HOS. The values of ' n ' ranges from 2–10 representing good adsorption, 1–2 moderate adsorption and less than one shows poor adsorption [82].

3.6.3. D-R model

The nonlinear form of D-R equation can be expressed as:

$$C_{\text{ads}} = C_m \exp(-\beta \varepsilon^2) \quad (16)$$

where C_m (mol/g) is the maximum amount of metal ions that can be adsorbed onto HOS under optimized experimental conditions, β is a constant related to adsorption energy and ε

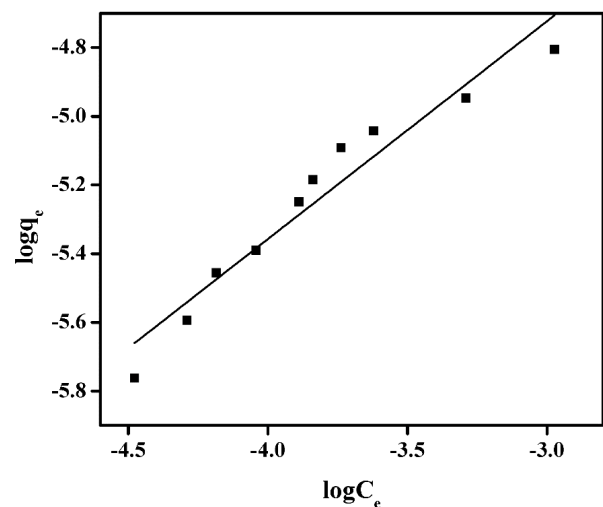


Fig. 17. Linear form of Freundlich isotherm for adsorption of Ni(II) onto husk of *Oryza sativa*.

(Polyanyi potential) = $RT \ln \left(1 + \frac{1}{C_e} \right)$ where R is the universal gas constant (kJ/mol K), T is the absolute temperature (K) and C_e is the equilibrium concentration of metal ions in solution (mol/g). The linearized form of D-R isotherm:

$$\ln C_{\text{ads}} = \ln C_m - \beta \varepsilon^2 \quad (17)$$

From β value, the mean adsorption energy (E) can be computed as [83]:

$$E = \frac{1}{\sqrt{-2\beta}} \quad (18)$$

which is the mean free energy of transfer of one mole of solute from infinity to the surface of adsorbent.

The plots of straight line were attained by employing linear form of D-R isotherm of Eq. (17) and are shown in Fig. 18. The values of C_m and β were measured from intercepts and slopes of plot of $\ln C_{\text{ads}}$ vs. ε^2 employing a least square fit program and are represented in Table 5. The D-R constants (C_m) for adsorption of Ni(II) onto HOS was

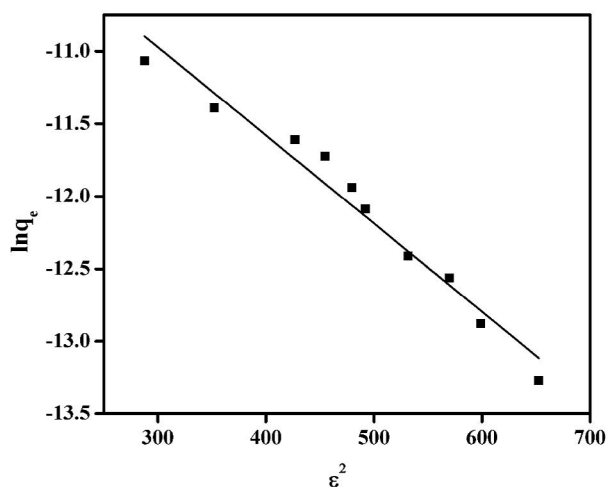


Fig. 18. Linear form of Dubinin Radushkevich (D-R) isotherm for adsorption of Ni(II) onto husk of *Oryza sativa*.

$(9.00 \pm 0.185) \times 10^{-5}$ mol/g calculated from intercept of straight lines employing least square fit program.

The value of β $(5.773 \pm 0.397) \times 10^{-3}$ was employed for calculating adsorption free energy (E) and measured E values for Ni(II) adsorption onto HOS was 9.28 ± 0.640 kJ/mol. The chemisorption phenomenon is operative for Ni(II) adsorption onto HOS.

Computer program Wavemetrics Igor Pro 6.2.1.2 was employed to measure D-R constants for nonlinear form using the plot of C_{ads} vs. C_e and are given in the Table 4 along with their respective (χ^2) values which can be employed as best fitting tool in nonlinear method. The values of ' C_m ' and ' β ' along with measured adsorption free energy are also given in Table 4. The nonlinear plots for adsorption of Ni(II) onto HOS are given in Fig. 15. Low numerical values of ' χ^2 ' for nonlinear and high values of ' R^2 ' for linear plots represents that experimental data followed well.

3.7. Adsorption thermodynamics

Thermodynamic investigations evaluate the feasibility and spontaneity of adsorption process. The endowments such as change in Gibb's free energy (ΔG°), enthalpy (ΔH°) and entropy (ΔS°) were calculated from below relations:

$$\ln K_c = \frac{\Delta S^\circ}{R} - \frac{\Delta H^\circ}{RT} \quad (19)$$

$$K_c = \frac{C_a}{C_e} \quad (20)$$

$$\Delta G^\circ = \Delta H^\circ - T\Delta S^\circ \quad (21)$$

where K_c , C_a , C_e , R , and T are equilibrium constant, amount of Ni(II) (mol/L) adsorbed onto adsorbent per litre (L) of solution at equilibrium, equilibrium concentration (mol/L) of Ni(II) in solution, general gas constant (8.31 J/mol K) and absolute temperature (K) respectively. Similarly ΔG° , ΔH° and ΔS° are change in Gibb's free energy (KJ/mol), enthalpy

(KJ/mol) and entropy (J/mol K) respectively. Fig. 19 represents the plot of $\ln K_c$ vs. $1/T$ for adsorption of Ni(II) onto HOS. The values of adsorption enthalpy (ΔH°) and entropy (ΔS°) for adsorption of Ni(II) onto HOS were calculated from slope and intercept of Fig. 19 and obtained results are given in Table 6. Similarly, the values of Gibb's free energy (ΔG°) for adsorption of Ni(II) onto HOS were also measured from Eq. (21) and are shown in Table 6. The values of Gibb's free energy (ΔG°) declines with rise in temperature representing the decrease in feasibility of adsorption at higher temperature. Moreover, the negative values of ΔG° for the adsorption of Ni(II) indicate that adsorption of Ni(II) is spontaneous in nature. The positive value of enthalpy (ΔH°) depicts that adsorption of Ni(II) onto HOS is an endothermic process. Similarly, the positive value of entropy (ΔS°) shows the enhancement in randomness at adsorbent-adsorbate interface during the adsorption Ni(II) onto HOS.

3.8. Applicability of procedure

The applicability of the developed procedure on real samples was checked by the removal of nickel ions from ordinary tap water sample using optimized conditions for adsorption. The removal efficiency of nickel ions were checked by spiking the sample with known amount of metal ions. Adsorption of Ni(II) ions from tap water sample were carried out in series of steps for achievement of maximum removal efficiency. HOS removed 83.9% of nickel ions, from spiked tap water sample in a single step whereas this percentage was increased up to 88.65%, by shaking the aliquot with the same weight of fresh adsorbent.

3.9. Recovery of adsorbed metal ions

The recovery of adsorbed metals and regeneration of the adsorbent are important aspects of wastewater treatment. Attempts were made to desorb the loaded metal ions from the HOS surface by using various desorbing media. For this purpose mineral acids such as hydrochloric, sulphuric, and

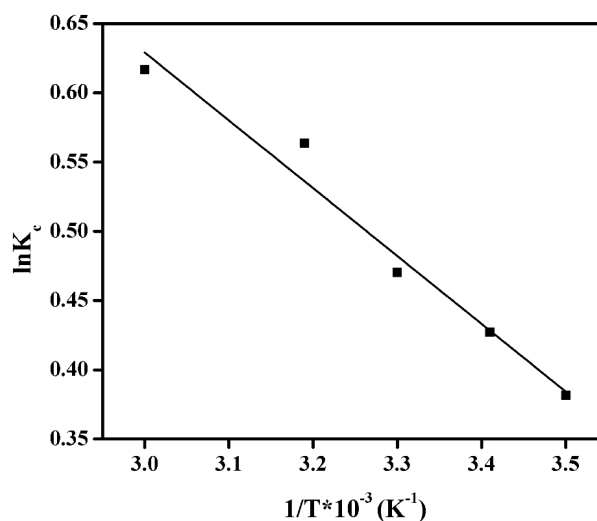


Fig. 19. Plot of $1/T$ vs. $\ln K_c$ for adsorption of Ni(II) onto husk of *Oryza sativa*.

Table 6
Thermodynamic parameters for adsorption of Ni(II) onto HOS

ΔH (KJ/mol)	ΔS (J/mol)	ΔG (KJ/mol)				
		283 K	293 K	303 K	313 K	333 K
4.10	17.44	-4.90	-5.10	-5.30	-5.50	-5.80

nitric acid solutions of different molarities were used by employing batch mode. For regeneration of nickel ions, fixed amount of metal loaded adsorbent was shaken with varied volumes and concentrations of HCl, H₂SO₄, and HNO₃ for specific time. Maximum recovery of adsorbed nickel onto HOS was attained with 0.1 mol/L HNO₃ solution.

4. Conclusions

Herein, batch adsorption of Ni(II) onto HOS from aqueous solution was evaluated at room temperature. The removal of Ni(II) was quantitative within a short contact time of 15 min without any prior chemical treatment or time consuming adjustments. The initial metal ions concentration for nickel was 3.4×10^{-4} mol/L. There was rapid increase in percent adsorption with initial time which slowed down as reaction proceeds until equilibrium was attained. The percentage of nickel ions increased from 42.99% to 62.32%. Adsorption kinetics studies showed that experimental data fitted well to pseudo-second-order kinetics. Adsorption isotherm analysis showed that experimental data fitted well to Langmuir isotherm model. Similarly thermodynamic study exhibited that adsorption of Ni(II) onto HOS was endothermic and spontaneous process. It indicated that HOS could be used as an excellent adsorbent for removal of Ni(II) from aqueous solution.

Acknowledgement

The authors are highly thankful to Higher Education Commission (HEC), Pakistan for financial support.

References

- [1] K.K. Deshmukh, Impact of human activities on the quality of groundwater from Sangamner Area, Ahmednagar District, Maharashtra, India, *Int. Res. J. Environ. Sci.*, 2 (2013).
- [2] Y. Sun, Q. Yue, B. Gao, Y. Gao, X. Xu, Q. Li, Y. Wang, Adsorption and cosorption of ciprofloxacin and Ni(II) on activated carbon-mechanism study, *J. Taiwan Inst. Chem. Eng.*, 45 (2014) 681–688.
- [3] Z. Zhou, D. Kong, H. Zhu, N. Wang, Z. Wang, Q. Wang, W. Liu, Q. Li, W. Zhang, Z. Ren, Preparation and adsorption characteristics of an ion-imprinted polymer for fast removal of Ni(II) ions from aqueous solution, *J. Hazard. Mater.*, 341 (2018) 355–364.
- [4] Y. Shi, T. Zhang, H. Ren, A. Kruse, R. Cui, Polyethylene imine modified hydrochar adsorption for chromium (VI) and nickel (II) removal from aqueous solution, *Bioresour. Technol.*, 247 (2018) 370–379.
- [5] Z. Guo, J. Zhang, H. Liu, Y. Kang, J. Yu, C. Zhang, Optimization of the green and low-cost ammoniation-activation method to produce biomass-based activated carbon for Ni(II) removal from aqueous solutions, *J. Cleaner Prod.*, 159 (2017) 38–46.
- [6] P. Burattin, M. Che, C. Louis, Molecular approach to the mechanism of deposition-precipitation of the Ni(II) phase on silica, *J. Phys. Chem. B*, 102 (1998) 2722–2732.
- [7] R.K. Singhal, J. Preeetha, R. Karpe, K. Tirumalesh, S.C. Kumar, A.G. Hegde, The use of ultrafiltration in trace metal speciation studies in sea water, *Environ. Int.*, 32 (2006) 224–228.
- [8] B. Wu, T. Christen, H.S. Tan, F. Hochstrasser, S.R. Suwarno, X. Liu, T.H. Chong, M. Burkhardt, W. Pronk, A.G. Fane, Improved performance of gravity-driven membrane filtration for seawater pretreatment: implications of membrane module configuration, *Water Res.*, 114 (2017) 59–68.
- [9] E. Pehlivan, T. Altun, Ion-exchange of Pb²⁺, Cu²⁺, Zn²⁺, Cd²⁺, and Ni²⁺ ions from aqueous solution by Lewatit CNP 80, *J. Hazard. Mater.*, 140 (2007) 299–307.
- [10] S. Suganya, P. Senthil Kumar, An investigation of adsorption parameters on ZVI-AC nanocomposite in the displacement of Se(IV) ions through CCD analysis, *J. Ind. Eng. Chem.*, 75 (2019) 211–223.
- [11] T.L. Marques, V.N. Alves, L.M. Coelho, N.M. Coelho, Removal of Ni(II) from aqueous solution using *Moringa oleifera* seeds as a bioadsorbent, *Water Sci. Technol.*, 65 (2012) 1435–1440.
- [12] M. Samarghandi, S. Azizian, M.S. Siboni, S. Jafari, S. Rahimi, Removal of divalent nickel from aqueous solutions by adsorption onto modified holly sawdust: equilibrium and kinetics, *Iran. J. Environ. Health Sci. Eng.*, 8 (2011) 167–174.
- [13] M. Rafatullah, O. Sulaiman, R. Hashim, A. Ahmad, Adsorption of copper (II), chromium (III), nickel (II) and lead (II) ions from aqueous solutions by meranti sawdust, *J. Hazard. Mater.*, 170 (2009) 969–977.
- [14] Y. Bulut, Z. Tez, Removal of heavy metals from aqueous solution by sawdust adsorption, *J. Environ. Sci.*, 19 (2007) 160–166.
- [15] R.H. Krishna, A. Swamy, Studies on the removal of Ni(II) from aqueous solutions using powder of mosambi fruit peelings as a low cost sorbent, *Chem. Sci. J.*, 31 (2011) 1–13.
- [16] N. Feng, X. Guo, S. Liang, Y. Zhu, J. Liu, Biosorption of heavy metals from aqueous solutions by chemically modified orange peel, *J. Hazard. Mater.*, 185 (2011) 49–54.
- [17] P.L. Homagai, K.N. Ghimire, K. Inoue, Adsorption behavior of heavy metals onto chemically modified sugarcane bagasse, *Bioresour. Technol.*, 101 (2010) 2067–2069.
- [18] M.V. Subbaiah, Y. Vijaya, N.S. Kumar, A.S. Reddy, A. Krishnaiah, Biosorption of nickel from aqueous solutions by *Acacia leucocephala* bark: kinetics and equilibrium studies, *Colloids Surf., B*, 74 (2009) 260–265.
- [19] M. Ajmal, R. Rao, J. Ahmad, R. Ahmad, The use of testa of groundnut shell (*Arachis hypogea*) for the adsorption of Ni(II) from the aqueous system, *J. Environ. Sci. Eng.*, 48 (2006) 221.
- [20] S. Suganya, K. Kayalvizhi, P. Senthil Kumar, A. Saravanan, V. Vinoth Kumar, Biosorption of Pb(II), Ni(II) and Cr(VI) ions from aqueous solution using *Rhizoclonium tortuosum*: extended application to nickel plating industrial wastewater, *Desal. Wat. Treat.*, 57 (2016) 25114–25139.
- [21] K.P.G.R. Gayathri, P. Senthil Kumar, S. Suganya, Adsorption capability of surface-modified jujube seeds for Cd(II), Cu(II) and Ni(II) ions removal: mechanism, equilibrium, kinetic and thermodynamic analysis, *Desal. Wat. Treat.*, 140 (2019) 268–282.
- [22] O. Olayinka, O. Oyedeji, A. Oyeyiola, Removal of chromium and nickel ions from aqueous solution by adsorption on modified coconut husk, *Afr. J. Environ. Sci. Technol.*, 3 (2009).
- [23] K.G. Bhattacharyya, J. Sarma, A. Sarma, *Azadirachta indica* leaf powder as a biosorbent for Ni(II) in aqueous medium, *J. Hazard. Mater.*, 165 (2009) 271–278.
- [24] S. Yadav, V. Srivastava, S. Banerjee, F. Gode, Y.C. Sharma, Studies on the removal of nickel from aqueous solutions using modified riverbed sand, *Environ. Sci. Pollut. Res.*, 20 (2013) 558–567.

- [25] T. Vengris, Nickel, copper and zinc removal from waste water by a modified clay sorbent, *Appl. Clay Sci.*, 18 (2001) 183–190.
- [26] R. Al Dwairi, A. Al-Rawajfeh, Removal of cobalt and nickel from wastewater by using Jordan low-cost zeolite and bentonite, *J. Univ. Chem. Technol. Metal.*, 41 (2012) 69–76.
- [27] K. Suresh, M. Borah, S. Jatty, Adsorption of nickel by bentonite clays. a comparative study, *J. Environ. Sci. Eng.*, 51 (2009) 133–136.
- [28] C.O. Ijagbemi, M.-H. Baek, D.-S. Kim, Montmorillonite surface properties and sorption characteristics for heavy metal removal from aqueous solutions, *J. Hazard. Mater.*, 166 (2009) 538–546.
- [29] S. Mukherjee, S. Kumar, A. Misra, P. Acharya, Removal of aqueous nickel (II) using laterite as a low-cost adsorbent, *Water Environ. Res.*, 78 (2006) 2268–2275.
- [30] A. Nezamzadeh-Ejehieh, M. Kabiri-Samani, Effective removal of Ni(II) from aqueous solutions by modification of nano particles of clinoptilolite with dimethylglyoxime, *J. Hazard. Mater.*, 260 (2013) 339–349.
- [31] R.R.V. Hemavathy, P.S. Kumar, S. Suganya, V. Swetha, S.J. Varjani, Modelling on the removal of toxic metal ions from aquatic system by different surface modified *Cassia fistula* seeds, *Bioresour. Technol.*, 281 (2019) 1–9.
- [32] P. Thamilarasu, K. Karunakaran, Removal of Ni(II) from aqueous solutions by adsorption onto Ricinus communis seed shell activated carbons, *J. Environ. Sci. Eng.*, 53 (2011) 7–14.
- [33] Y. Onundi, A. Mamun, M. Al Khatib, Y. Ahmed, Adsorption of copper, nickel and lead ions from synthetic semiconductor industrial wastewater by palm shell activated carbon, *Int. J. Environ. Sci. Technol.*, 7 (2010) 751–758.
- [34] H. Kalavathy, B. Karthik, L.R. Miranda, Removal and recovery of Ni and Zn from aqueous solution using activated carbon from *Hevea brasiliensis*: batch and column studies, *Colloids Surf., B*, 78 (2010) 291–302.
- [35] M.A. Adolph, Y.M. Xavier, P. Kriveshini, K. Rui, Phosphine functionalised multiwalled carbon nanotubes: a new adsorbent for the removal of nickel from aqueous solution, *J. Environ. Sci.*, 24 (2012) 1133–1141.
- [36] H. Lata, V. Garg, R. Gupta, Sequestration of nickel from aqueous solution onto activated carbon prepared from *Parthenium hysterophorus* L, *J. Hazard. Mater.*, 157 (2008) 503–509.
- [37] S. Yang, J. Li, D. Shao, J. Hu, X. Wang, Adsorption of Ni(II) on oxidized multi-walled carbon nanotubes: Effect of contact time, pH, foreign ions and PAA, *J. Hazard. Mater.*, 166 (2009) 109–116.
- [38] M.I. Khan, S. Zafar, H.B. Ahmad, M. Hussain, Z. Shafiq, Use of morus alba leaves as bioadsorbent for the removal of congo red dye, *Fresenius Environ. Bull.*, 24 (2015) 2251–2258.
- [39] M.I. Khan, S. Zafar, M.A. Khan, F. Mumtaz, P. Prapamonthon, A.R. Buzdar, *Bougainvillea glabra* leaves for adsorption of congo red from wastewater, *Fresenius Environ. Bull.*, 27 (2018) 1456–1465.
- [40] M.I. Khan, S. Zafar, A.R. Buzdar, M.F. Azhar, W. Hassan, A. Aziz, Use of citrus sinensis leaves as a bioadsorbent for removal of congo red dye from aqueous solution *Fresenius Environ. Bull.*, 27 (2018) 4679–4688.
- [41] M.I. Khan, S. Zafar, M.F. Azhar, A.R. Buzdar, W. Hassan, A. Aziz, M. Khraisheh, Leaves powder of syzgium cumini as an adsorbent for removal of congo red dye from aqueous solution, *Fresenius Environ. Bull.*, 27 (2018) 3342–3350.
- [42] M.A. Khan, M.I. Khan, S. Zafar, Removal of different anionic dyes from aqueous solution by anion exchange membrane, *Membr. Water Treat.*, 8 (2016) 259–277.
- [43] M.I. Khan, L. Wu, A.N. Mondal, Z. Yao, L. Ge, T. Xu, Adsorption of methyl orange from aqueous solution on anion exchange membranes: adsorption kinetics and equilibrium, *Membr. Water Treat.*, 7 (2016) 23–38.
- [44] M.I. Khan, M.A. Khan, S. Zafar, M.N. Ashiq, M. Athar, A.M. Qureshi, M. Arshad, Kinetic, equilibrium and thermodynamic studies for the adsorption of methyl orange using new anion exchange membrane (BII), *Desal. Wat. Treat.*, 58 (2016) 285–297.
- [45] M.I. Khan, M.A. Khan, A.R. Buzdar, P. Prapamonthon, Adsorption kinetic, equilibrium and thermodynamic study for the removal of Congo Red from aqueous solution, *Desal. Wat. Treat.*, 98 (2017) 294–305.
- [46] M.I. Khan, T.M. Ansari, S. Zafar, A.R. Buzdar, M.A. Khan, F. Mumtaz, P. Prapamonthon, M. Akhtar, Acid green-25 removal from wastewater by anion exchange membrane: adsorption kinetic and thermodynamic studies, *Membr. Water Treat.*, 9 (2018) 79–85.
- [47] M.I. Khan, S. Akhtar, S. Zafar, A. Shaheen, M.A. Khan, R. Luque, Removal of Congo Red from aqueous solution by anion exchange membrane (EBTAC): adsorption kinetics and thermodynamics, *Materials*, 8 (2015) 4147–4161.
- [48] S. Zafar, M.I. Khan, M. Khraisheh, S. Shahida, T. Javed, M.L. Mirza, N. Khalid, Use of rice husk as an effective sorbent for the removal of cerium ions from aqueous solution: kinetic, equilibrium and thermodynamic studies, *Desal. Wat. Treat.*, 150 (2019) 124–135.
- [49] S. Zafar, M.I. Khan, M. Khraisheh, S. Shahida, N. Khalid, M.L. Mirza, Effective removal of lanthanum ions from aqueous solution using rice husk: impact of experimental variables, *Desal. Wat. Treat.*, 132 (2019) 263–273.
- [50] A. Demirbas, Heavy metal adsorption onto agro-based waste materials: a review, *J. Hazard. Mater.*, 157 (2008) 220–229.
- [51] D.W. O'Connell, C. Birkinshaw, T.F. O'Dwyer, Heavy metal adsorbents prepared from the modification of cellulose: a review, *Bioresour. Technol.*, 99 (2008) 6709–6724.
- [52] S. Zafar, N. Khalid, M.L. Mirza, Potential of rice husk for the decontamination of silver ions from aqueous media, *Sep. Sci. Technol.*, 47 (2012) 1793–1801.
- [53] E. Repo, T.A. Kurniawan, J.K. Warchol, M.E. Sillanpaa, Removal of Co(II) and Ni(II) ions from contaminated water using silica gel functionalized with EDTA and/or DTPA as chelating agents, *J. Hazard. Mater.*, 171 (2009) 1071–1080.
- [54] S. Dahiya, R.M. Tripathi, A.G. Hegde, Biosorption of heavy metals and radionuclide from aqueous solutions by pre-treated arca shell biomass, *J. Hazard. Mater.*, 150 (2008) 376–386.
- [55] S. Yadav, V. Srivastava, S. Banerjee, F. Gode, Y.C. Sharma, Studies on the removal of nickel from aqueous solutions using modified riverbed sand, *Environ. Sci. Pollut. Res. Int.*, 20 (2013) 558–567.
- [56] M.I. Din, M.L. Mirza, Biosorption potentials of a novel green biosorbent Saccharum bengalense containing cellulose as carbohydrate polymer for removal of Ni(II) ions from aqueous solutions, *Int. J. Biol. Macromol.*, 54 (2013) 99–108.
- [57] D.K.V. Ramana, D.H.K. Reddy, B.N. Kumar, Y. Harinath, K. Seshiah, Removal of nickel from aqueous solutions by citric acid modified *Ceiba Pentandra* hulls: equilibrium and kinetic studies, *Can. J. Chem. Eng.*, 90 (2012) 111–119.
- [58] K.A. Krishnan, K.G. Sreejalekshmi, R.S. Baiju, Nickel(II) adsorption onto biomass based activated carbon obtained from sugarcane bagasse pith, *Bioresour. Technol.*, 102 (2011) 10239–10247.
- [59] P.E. Aikpokpodion, R.R. Ipinmoroti, S.M. Omotoso, Biosorption of nickel (II) from aqueous solution using waste tea (*Camellia cinensis*) materials, *Am.-Eurasian J. Toxicol. Sci.*, 2 (2010) 72–82.
- [60] V.C. Srivastava, I.D. Mall, I.M. Mishra, Competitive adsorption of cadmium(II) and nickel(II) metal ions from aqueous solution onto rice husk ash, *Chem. Eng. Process*, 48 (2009) 370–379.
- [61] M. Bansal, D. Singh, V.K. Garg, P. Rose, Use of agricultural waste for the removal of nickel ions from aqueous solutions: equilibrium and kinetics studies, *Int. J. Civ. Environ. Eng.*, 1 (2009) 108–114.
- [62] X. Zhang, X. Wang, Adsorption and desorption of nickel (II) ions from aqueous solution by a lignocellulose/montmorillonite nanocomposite, *PLoS One*, 10 (2015) e0117077.
- [63] S. Suganya, A. Saravanan, P. Senthil Kumar, M. Yashwanthraj, P. Sundar Rajan, K. Kayalvizhi, Sequestration of Pb(II) and Ni(II) ions from aqueous solution using microalga *Rhizoclonium hookeri*: adsorption thermodynamics, kinetics, and equilibrium studies, *J. Water Reuse Desal.*, 7 (2017) 214–227.
- [64] S. Zafar, N. Khalid, M.L. Mirza, Sequestering of thorium ions from aqueous media on rice husk: equilibrium, kinetic and thermodynamic studies, *Radiachim. Acta*, 103 (2015) 385–395.
- [65] S.K. Kazy, S. D'Souza, P. Sar, Uranium and thorium sequestration by a *Pseudomonas* sp.: mechanism and chemical characterization, *J. Hazard. Mater.*, 163 (2009) 65–72.

- [66] V.C. Srivastava, I.D. Mall, I.M. Mishra, Characterization of mesoporous rice husk ash (RHA) and adsorption kinetics of metal ions from aqueous solution onto RHA, *J. Hazard. Mater.*, 134 (2006) 257.
- [67] S.K. Kazy, P. Sar, S.P. Singh, A.K. Sen, S.F. D'Souza, Extracellular polysaccharides of a copper sensitive and a copper resistant *Pseudomonas aeruginosa* strain: synthesis, chemical nature and copper binding, *World J. Microbiol. Biotechnol.*, 18 (2002) 583.
- [68] Y.-M. Xu, J. Qi, D.-M. He, D.-M. Wang, H.-Y. Chen, J. Guan, Q.-M. Zhang, Preparation of amorphous silica from oil shale residue and surface modification by silane coupling agent, *Oil Shale*, 27 (2010) 37–46.
- [69] L. Ludueña, D. Fasce, V.A. Alvarez, P.M. Stefani, Nanocellulose from rice husk following alkaline treatment to remove silica, *BioResources*, 6 (2011) 1440–1453.
- [70] S. Suganya, P.S. Kumar, A. Saravanan, P.S. Rajan, C. Ravikumar, Computation of adsorption parameters for the removal of dye from wastewater by microwave assisted sawdust: theoretical and experimental analysis, *Environ. Toxicol. Pharmacol.*, 50 (2017) 45–57.
- [71] M.B. Ibrahim, W.L. Jimoh, Bioremediation of Ni(II) and Cd(II) from aqueous solution, *Indian J. Sci. Technol.*, 4 (2011) 487–491.
- [72] H. Omar, S. Abu-Kharda, L. Abd El-Baset, R. Abu-Shohba, Efficiency of dry (*Psidium guava*) leaves for the removal of cesium-137 from aqueous solutions, *Arabian J. Nucl. Sci. Appl.*, 45 (2012) 505–515.
- [73] J.T. Nwabanne, P.K. Igbokwe, Copper (II) uptake by adsorption using palmyra palm nut, *Adv. Appl. Sci. Res.*, 2 (2011) 166–175.
- [74] M. Torab-Mostaedi, Biosorption of lanthanum and cerium from aqueous solutions using tangerine (*Citrus reticulata*) peel: equilibrium, kinetic, and thermodynamic studies, *Chem. Ind. Chem. Eng.*, 19 (2013) 79–88.
- [75] S. Ho Lee, C. Hun Jung, H. Chung, M. Yeal Lee, J.-W. Yang, Removal of heavy metals from aqueous solution by apple residues, *Process Biochem.*, 33 (1998) 205–211.
- [76] R. Gao, J. Wang, Effects of pH and temperature on isotherm parameters of chlorophenols biosorption to anaerobic granular sludge, *J. Hazard. Mater.*, 145 (2007) 398–403.
- [77] G. Yan, T. Viraraghavan, Effect of pretreatment on the bio-adsorption of heavy metals on *Mucor rouxii*, *Water SA-Pretoria*, 26 (2000) 119–124.
- [78] N. Kannan, M.M. Sundaram, Kinetics and mechanism of removal of methylene blue by adsorption on various carbons—a comparative study, *Dyes Pigm.*, 51 (2001) 25–40.
- [79] E. Tütem, R. Apak, Ç.F. Ünal, Adsorptive removal of chlorophenols from water by bituminous shale, *Water Res.*, 32 (1998) 2315–2324.
- [80] I.D. Mall, V.C. Srivastava, N.K. Agarwal, I.M. Mishra, Adsorptive removal of malachite green dye from aqueous solution by bagasse fly ash and activated carbon-kinetic study and equilibrium isotherm analyses, *Colloids Surf., A*, 264 (2005) 17–28.
- [81] I. Langmuir, The adsorption of gases on plane surfaces of glass, mica, and platinum, *J. Am. Chem. Soc.*, 40 (1918) 1361–1403.
- [82] B. Subramanyam, A. Das, Linearized and non-linearized isotherm models comparative study on adsorption of aqueous phenol solution in soil, *Int. J. Environ. Sci. Technol.*, 6 (2009) 633–640.
- [83] A. Itodo, H. Itodo, Sorption energies estimation using Dubinin-Radushkevich and Temkin adsorption isotherms, *Life Sci. J.-Acta Zhengzhou Uni.*, 7 (2010) 31–39.